Robust Resource Allocation for RIS-aided V2X Communications with Imperfect CSI

Weihua Wu, Peng Wang, Yue Fan, Jiayi Liu, Runzi Liu, and Wenchao Xia

***Abstract*—This paper investigates a robust resource allocation for reconfigurable intelligent surface (RIS) aided vehicle-to-everything (V2X) communications with imperfect channel state information (CSI). To satisfy the diverse quality-of-service (QoS) requirements of V2X communications, we aim at maximizing the sum capacity of cellular user equipments (CUEs) while guaranteeing the outage probability constraints of vehicular user equipments (VUEs). Then, the considered problem is decomposed into the subproblems of power, spectrum and RIS phase shift optimization. A graph-based power allocation method is presented to transform the non-convex power allocation subproblem into a tractable one and obtain the closed-form solutions. A worst-case conditional value-at-risk (CVaR) approximation-based method is developed to convert the RIS phase optimization subproblem into a convex semidefinite programming (SDP) problem. We propose a low-complexity learning-based alternating optimization approach which alternately optimizes three subproblems to obtain a near-optimal solution. Simulation results demonstrate that the proposed approach outperforms other benchmark methods.**

***Key Terms*: V2X communications, RIS, robust resource allocation, outage probability constraint, uncertain channel.**

I. Introduction

In recent years, vehicle-to-everything (V2X) communications, including vehicle-to-infrastructure (V2I) and vehicle-to-vehicle (V2V) communications, have gained increasing interest due to their potential to tackle traffic-related issues, such as road safety and traffic efficiency, etc [1]. However, the propagation quality of V2X communication links is often degraded because of the rapidly varying channels caused by the high mobility of vehicles and the complexity of the urban communication environment, such as high buildings blocking the channels [2]. To enhance the propagation quality, reconfigurable intelligent surface (RIS) is emerging as a promising transmission technology that can reconfigure the wireless channel as well as improve energy efficiency [3]. Specifically, RIS is invented to reflect the signal from the base station (BS) to a targeted user for enhancing received signal quality or restrain the interference, thereby ensuring security and privacy [4]. Compared with conventional active antennas equipped with energy-inefficient radio frequency (RF) chains and power amplifiers, RIS with passive reflective elements are more cost-effective and energy-efficient [5]. Hence, these advantages make RIS a potential technology to enhance the performance of the vehicular wireless communication systems.

Resource allocation for RIS-aided wireless communication networks has been extensively explored in many research fields. However, there are still significant gaps in the research on RIS-aided vehicular communications. In [6], a resource allocation problem based on RIS-aided vehicle networks was solved by jointly optimizing the power allocation, the spectrum allocation and the RIS reflection coefficients. The authors in [7] studied a RIS resource allocation problem, joint power allocation of device-to-device (D2D) nodes and RIS passive beam forming in RIS-based D2D communication networks. The work in [8] proposed a block coordinate descent (BCD) method to solve a spectrum allocation problem in RIS supported vehicle systems. However, none of the above methods consider the channel uncertainties caused by the limited channel feedback, partial channel state information (CSI) acquisition and the Doppler effect [9]. Therefore, these works failed to guarantee the outage probability constraint, leading to the violation of the quality-of-service (QoS) constraints for communication links. To guarantee the QoS constraints, [10] developed a semidefinite relaxation (SDR)-based BCD approach to research a joint optimization problem in D2D networks where the CSI is imperfect. The work in [11] proposed an alternate optimization (AO) method to resolve the transmit power minimization problem where the chance constraint is based on the statistical CSI error model. In [12], the authors applied Bernstein-type inequality and SDR to transform a minimum transmit power optimization problem into a semidefinite programming (SDP) problem for RIS-aided communications based on the statistical CSI error model. However, these works assume that the CSI is based on a known probability distribution model, such as the statistical error model and the bounded error model, rather than an unknown probability distribution model.

Against the above background, we research the robust resource allocation for RIS-aided V2X communications, considering the CSI of the unknown distribution of the partial vehicular channels. Then, a joint power allocation, spectrum allocation and RIS phase shift optimization problem is designed

*This work was supported in part by the NSF China under Grant 61801365; in part by the Natural Science Basic Research Program of Shaanxi under Grant 2023-JC-YB-542 and 2023-JC-YB-566; and in part by the Young Talent fund of University Association for Science and Technology in Shaanxi under Grant 20200112.

W. Wu is with the School of Physics and Information Technology, Shaanxi Normal University, Xi'an 710119, China (email:whwu@snnu.edu.cn).

P. Wang, Y. Fan and J. Liu are with State Key Laboratory of ISN, School of Telecommunications Engineering, Xidian University, No.2 South Taibai Road, Xi'an, 710071, Shaanxi, China (email:wangp134@163.com; fanyue5408@163.com; jyliu@xidian.edu.cn).

R. Liu is with the School of Information and Control Engineering, Xi'an University of Architecture and Technology, Xi'an 710055, China (email:rz_liu@126.com).

W. Xia is with Jiangsu Key Laboratory of Wireless Communications, Nanjing University of Posts and Telecommunications, Nanjing 210003, China (e-mail: xiawenchao@njupt.edu.cn).

979-8-3503-2928-5/23/$31.00 ©2023 IEEE

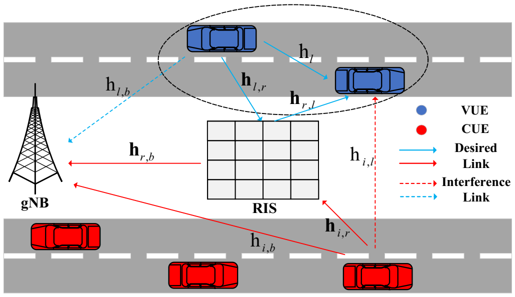

Fig. 1. RIS-aided single cellular vehicle communications

to maximize the sum capacity of cellular user equipments (CUEs) while guaranteeing the outage probability constraints of vehicular user equipments (VUEs) and the unit-modulus constraint of RIS. We decompose the considered problem into three subproblems and develop a low-complexity learning-based alternating optimization approach, which alternately optimizes them to obtain a near-optimal solution.

II. System Model

A. Network Model

As shown in Fig. 1, we consider an RIS-aided single cellular vehicle network based on V2X communications, which consists of one gNB, one RIS and some vehicles. We consider a single-input single-output (SISO) uplink communication network, where both the Next Generation NodeB (gNB) and the vehicles are equipped with a single antenna. There are I CUEs communicating via V2I links and L VUE pairs achieving V2V communication, denoted as $\mathcal{I}=\{1,2,\cdots,I\}$ and $\mathcal{L}=\{1,2,\cdots,L\}$, respectively. In mode-1, the orthogonal resource blocks (RBs) are allocated to CUEs by the gNB. Since CUEs utilize the uplink resources sparsely and VUEs generally generate minor interference to gNB, the uplink resources of CUEs can be reused by VUE pairs. The binary variable $z_{i,l}$ is applied to represent the allocation of uplink resources for CUE. If the spectrum of the ith CUE is reused by the lth VUE, $z_{i,l}=1$. Otherwise, $z_{i,l}=0$. P_i^c and P_l^d represent the transmit power of the ith CUE and the transmitter of the lth VUE pair, respectively. The RIS consists of R reflecting elements defined as $\mathcal{R}=\{1,2,\cdots,R\}$, which can adjust the channel by optimizing their phase shifts. The phase shift matrix is represented by $\mathbf{E}=diag\left([e_1,\cdots,e_R]\right)$, where $e_r=e^{j\varphi_r}$ and φ_r is the phase shift of the rth element.

The channel gain from the ith CUE to the gNB is modelled as $h_{i,b}=\sqrt{\omega_{i,b}}\tilde{h}_{i,b}=\sqrt{\lambda d_{i,b}^{\beta_{i,b}}}\tilde{h}_{i,b}$, where $\omega_{i,b}$ denotes the large-scale slow fading channel gain, $\tilde{h}_{i,b}$ is the small-scale fast fading gain, λ is the pathloss at the distance of 1 metre, d is the link distance in metres and β is the pathloss exponent. Similarly, the definitions of the channel gain $\mathbf{h}_{i,r}\in\mathbb{C}^{R\times1}$, $\mathbf{h}_{r,b}\in\mathbb{C}^{R\times1}$, $\mathbf{h}_{l,r}\in\mathbb{C}^{R\times1}$, $\mathbf{h}_{r,l}\in\mathbb{C}^{R\times1}$, h_l as well as the crosstalk channel gain $h_{i,l}$ and $h_{l,b}$ are similar to $h_{i,b}$. Since the large-scale fading components are generally influenced by the position of vehicles and vary on a slow scale, gNB has the ability to perfectly obtain the pathloss exponent and the link distance of all links. However, for the small-scale fading, we consider different assumptions for different channels. As the gNB has sensing capability, the CSI can be accurately obtained by the gNB for channels directly connected to the gNB, i.e., $\tilde{h}_{i,b}$ and $\tilde{h}_{l,b}$, as well as for cascaded channels whose final destination is the gNB, i.e., $\tilde{\mathbf{h}}_{i,r}$, $\tilde{\mathbf{h}}_{l,r}$ and $\tilde{\mathbf{h}}_{r,b}$. For the channels whose destinations are vehicles, i.e., $\tilde{h}_l$, $\tilde{h}_{i,l}$ and $\tilde{\mathbf{h}}_{r,l}$, we assume that the gNB can only obtain the estimated channel fading $\bar{h}$ with error $\hat{h}$, due to the Doppler effect generated by the high mobility of vehicles. We apply a first-order Gauss-Markov process [13] to model the small-scale channel fading of the vehicular links as

$$\tilde{h}=\kappa\bar{h}+\sqrt{1-\kappa^2}\hat{h},$$

where $\hat{h}\sim\mathcal{CN}(0,1)$ is independent and identically distributed (i.i.d.) and κ $(0<\kappa<1)$ denotes the channel correlated coefficient at two successive time intervals.

Herein, the received signal-to-interference-plus-noise ratio (SINR) at the gNB and the receiver of the lth VUE can be expressed as

$$\gamma_i=\frac{P_i^c h_i^B}{\sum\limits_{l\in\mathcal{L}} z_{i,l}P_l^d h_l^B+\sigma^2}=\frac{P_i^c\left|h_{i,b}+\mathbf{h}_{r,b}^H\mathbf{E}\mathbf{h}_{i,r}\right|^2}{\sum\limits_{l\in\mathcal{L}} z_{i,l}P_l^d\left|h_{l,b}+\mathbf{h}_{r,b}^H\mathbf{E}\mathbf{h}_{l,r}\right|^2+\sigma^2},$$

and

$$\gamma_l=\frac{P_l^d h_l^d}{\sum\limits_{i\in\mathcal{I}} z_{i,l}P_i^c h_i^d+\sigma^2}=\frac{P_l^d\left|h_l+\mathbf{h}_{r,l}^H\mathbf{E}\mathbf{h}_{l,r}\right|^2}{\sum\limits_{i\in\mathcal{I}} z_{i,l}P_i^c\left|h_{i,l}+\mathbf{h}_{r,l}^H\mathbf{E}\mathbf{h}_{i,r}\right|^2+\sigma^2},$$

respectively, where σ^2 is the power of noise.

B. Problem Formulation

To guarantee the requirements of high-data rate mobile services and ultra-reliable data transmission services, the sum capacity of CUEs is maximized while satisfying the outage probability requirement of VUEs due to the uncertain CSI of the vehicle links. On this basis, the resource allocation problem involves the joint optimization of the transmit power $\mathbf{P}=\left\{P_i^c,P_l^d,\forall i,l\right\}$, the allocation of spectrum resources $\mathbf{Z}=\{z_{i,l},\forall i,l\}$ and the RIS phase shift matrix $\mathbf{E}$. Hence, the problem is formulated as

$$\max_{\{\mathbf{P},\mathbf{E},\mathbf{Z}\}}\sum_{i\in\mathcal{I}}W\log_2(1+\gamma_i) \tag{1}$$

$$\text{s.t.}\quad \Pr\{\gamma_l\geq\gamma_{th}\}\geq1-\delta,\forall l\in\mathcal{L}, \tag{1a}$$

$$|e_r|=1,\ \forall r\in\mathcal{R}, \tag{1b}$$

$$\sum_{l\in\mathcal{L}}z_{i,l}=1,\forall i\in\mathcal{I},\sum_{i\in\mathcal{I}}z_{i,l}=1,\forall l\in\mathcal{L}, \tag{1c}$$

$$z_{i,l}\in\{0,1\},\forall i\in\mathcal{I},l\in\mathcal{L}, \tag{1d}$$

$$0\leq P_i^c\leq P_i^{\max},\forall i\in\mathcal{I},0\leq P_l^d\leq P_l^{\max},\ \forall l\in\mathcal{L}, \tag{1e}$$

where W is the bandwidth of spectrum resources, γ_{th} is the minimum SINR requirement for V2V communication, δ is the maximum tolerable outage probability for V2V communication, $P_i^{\max}$ and $P_l^{\max}$ are the maximum transmit power for CUEs and VUEs. More specifically, (1b) ensures the unit-modulus constraint on the phase shift of each RIS reflecting element. (1c) characterizes that the spectrum of one CUE can only be reused by one VUE pair and one VUE can only reuse the spectrum of one CUE. Because the variables are coupled with each other and the variable $z_{i,l}$ is binary variable, the resource allocation problem in (1) is a mixed-integer non-convex problem. To solve this non-convex problem, a learning-based alternating optimization approach is proposed.

III. Learning-based Alternating Optimization Approach

In this section, we present a learning-based alternating optimization approach (LAOA) to solve problem (1). Since there are three variables $\mathbf{P}$, $\mathbf{E}$ and $\mathbf{Z}$ which are coupled with each other, it is difficult to find an efficient allocation to optimize three variables and obtain the globally optimal solution. In the following, we employ the AO approach to decompose problem (1) into three subproblems, i.e., the spectrum allocation subproblem, the power allocation subproblem and the phase shift optimization subproblem, and then alternately optimize them while fixing the other variables.

A. Power Allocation Subproblem

For transforming the outage probability constraint in (1a), we propose a learning method that applies a high probability region (HPR) to represent the uncertain CSI of the vehicular channels. In order to acquire the HPR, we should collect multiple samples of the uncertain CSI and learn the uncertain set, which must cover all samples with the probability $1-\delta$. If the acquired power solution is feasible under the $1-\delta$ content of uncertain samples, the outage probability constraint must be satisfied. Inspired by this thought, when the spectrum allocation $\mathbf{Z}$ and the phase shift matrix $\mathbf{E}$ are given, the approximate form of the power allocation subproblem can be formulated as

$$C_{i,l} = \max_{\mathbf{P}} \quad W\log_2\left(1+\frac{P_i^c h_i^B}{P_l^d h_l^B+\sigma^2}\right) \tag{2}$$

$$\text{s.t.} \quad \mathbf{p}_l^d \boldsymbol{\theta}_l^d \geq \sigma^2, \boldsymbol{\theta}_l^d \in \mathbf{H}_l^d, \tag{2a}$$

$$0 \leq P_i^c \leq P_i^{\max},\ 0 \leq P_l^d \leq P_l^{\max}, \tag{2b}$$

where $\mathbf{p}_l^d = [\frac{P_l^d}{\gamma_{th}}, -P_i^c]$, $\boldsymbol{\theta}_l^d = [h_l^d, h_i^d]^T$ and $\mathbf{H}_l^d$ is the HPR. When $\mathbf{H}_l^d$ cover all samples of uncertain CSI $\boldsymbol{\theta}_l^d$ with the probability $1-\delta$, the feasible solutions of (2) must satisfy

$$\Pr\{\gamma_l \geq \gamma_{th}\} \geq \Pr\{\boldsymbol{\theta}_l^d \in \mathbf{H}_l^d\} \geq 1-\delta. \tag{3}$$

Since the affine set can simplify the intractable problem, the HPR is modeled as $\mathbf{H}_l^d = \left\{\boldsymbol{\theta}_s^d \middle| \tilde{\mathbf{p}}_l^d \boldsymbol{\theta}_l^d \geq r_l\right\}$, where $\tilde{\mathbf{p}}_l^d = [\frac{\tilde{P}_l^d}{\gamma_{th}}, -\tilde{P}_i^c]$ is a given initial feasible solution and r_l is the size of the HPR. For learning the size r_l, M i.i.d. samples of the uncertain CSI $\boldsymbol{\theta}_l^d$ are collected as $\mathcal{M} = \{\boldsymbol{\eta}_1, \boldsymbol{\eta}_2, \cdots, \boldsymbol{\eta}_M\}$, where $\boldsymbol{\eta}_m \in \mathbb{R}^2$. Let $k(\boldsymbol{\eta}_m) = \tilde{\mathbf{p}}_l^d \boldsymbol{\eta}_m$ be the map from the random space $\mathbb{R}^2$ into $\mathbb{R}$. Then, the values $k(\boldsymbol{\eta}_m)$ of all samples in $\mathcal{M}$ can be computed and sorted in ascending order $k^{(1)}(\boldsymbol{\eta}) \leq \cdots \leq k^{(M)}(\boldsymbol{\eta})$. The $(1-\delta)$-quantile $q_{1-\delta}$ is introduced as

$$\Pr\{k(\boldsymbol{\eta}) \leq q_{1-\delta}\} = 1-\delta. \tag{4}$$

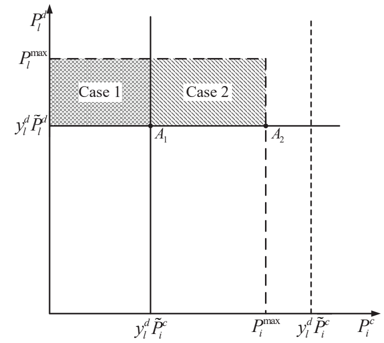

Fig. 2. Two cases in the feasible region of problem (2).

Hence, the size of the HPR can be learned as the upper bound of $(1-\delta)$-quantile of $k(\boldsymbol{\eta})$, which is considered as $r_l = k^{\lceil(1-\delta)M\rceil}(\boldsymbol{\eta})$.

Based on the learned $\mathbf{H}_l^d$, for satisfying the outage constraint of V2V links, we need compute the minimum $\boldsymbol{\theta}_l^d$ of (2a) via the following optimization

$$\min_{\boldsymbol{\theta}_l^d} \ \mathbf{p}_l^d \boldsymbol{\theta}_l^d \quad \text{s.t.} \quad \tilde{\mathbf{p}}_l^d \boldsymbol{\theta}_l^d \geq r_l. \tag{5}$$

Then, the dual problem of (5) is

$$\max_{y_l^d} \ y_l^d r_l \quad \text{s.t.} \ y_l^d \tilde{\mathbf{p}}_l^d \leq \mathbf{p}_l^d, y_l^d \geq 0. \tag{6}$$

According to above transformation, after vector $\tilde{\mathbf{p}}_l^d$ and $\mathbf{p}_l^d$ are decomposed into the scalar form, the outage constraint is converted into the linear constraints as follows

$$y_l^d r_l \geq \sigma^2, y_l^d \geq 0, y_l^d \tilde{P}_l^d \leq P_l^d, y_l^d \tilde{P}_i^c \geq P_i^c. \tag{7}$$

Then, by combining (2b) with (7), the power allocation subproblem can be reformulated as

$$C_{i,l} = \max_{\mathbf{P}} \ W\log_2\left(1+\frac{P_i^c h_i^B}{P_l^d h_l^B+\sigma^2}\right) \tag{8}$$

$$\text{s.t.} \ 0 \leq P_i^c \leq \min\left\{y_l^d \tilde{P}_i^c, P_i^{\max}\right\}, y_l^d \tilde{P}_l^d \leq P_l^d \leq P_l^{\max}, \tag{8a}$$

$$y_l^d r_l \geq \sigma^2, y_l^d \geq 0. \tag{8b}$$

Based on the constraints of (8), we can construct the feasible region of problem (8) as shown in Fig. 2. According to analysing the values of $y_l^d \tilde{P}_i^c$ and $P_i^{\max}$, we can discuss the power solution in following two cases.

1) Case 1: When $y_1^d \tilde{P}_i^c \leq P_i^{\max}$, the feasible region satisfies Case 1 in Fig. 2. From the objective function of problem (8), we observe that the capacity increases monotonically with P_i^c when P_l^d is fixed. On the contrary, the capacity decreases monotonically with P_l^d when P_i^c is fixed. Therefore, the optimal value of problem (8) must be located in A_1. When we substitute the coordinate of A_1 $(y_l^d \tilde{P}_i^c, y_l^d \tilde{P}_l^d)$ into the objective function, we observe that the objective function becomes the function of y_1^d and monotonically increases with y_1^d. The feasible region of y_1^d can be obtained as $\frac{\sigma^2}{r_l} \leq y_1^d \leq \min\{\frac{P_l^{\max}}{\tilde{P}_l^d}, \frac{P_i^{\max}}{\tilde{P}_i^c}\}$, so the optimal value is $y_1^{d,*} = \min\{\frac{P_l^{\max}}{\tilde{P}_l^d}, \frac{P_i^{\max}}{\tilde{P}_i^c}\}$.

2) Case 2: When $y_1^d \tilde{P}_i^c \geq P_i^{\max}$, the feasible region satisfies Case 2 in Fig. 2. Similarly, the optimal value of problem (8) must be located in A_2. Then, when we substitute the coordinate of A_2 into the objective function, we find the objective function monotonically decreases with y_1^d and the feasible region of y_1^d is $\max\{\frac{\sigma^2}{r_l},\frac{P_i^{\max}}{\tilde{P}_i^c}\}\le y_1^d\le\frac{P_l^{\max}}{\tilde{P}_l^d}$. Hence, the optimal value is $y_1^{d,*}=\max\{\frac{\sigma^2}{r_l},\frac{P_i^{\max}}{\tilde{P}_i^c}\}$.

To sum up, when we substitute $y_1^{d,*}$ into the coordinate of A_1 and A_2, the closed-form solution of the power allocation subproblem can be obtained as

$$C_{i,l}(P_i^{c,*},P_l^{d,*})=\begin{cases}(\frac{P_l^{\max}\tilde{P}_i^c}{\tilde{P}_l^d},P_l^{\max}),\text{if}\frac{\sigma^2}{r_l}\le\frac{P_l^{\max}}{\tilde{P}_l^d}\le\frac{P_i^{\max}}{\tilde{P}_i^c},\\(P_i^{\max},\frac{P_i^{\max}\tilde{P}_l^d}{\tilde{P}_i^c}),\text{if}\frac{\sigma^2}{r_l}\le\frac{P_i^{\max}}{\tilde{P}_i^c}\le\frac{P_l^{\max}}{\tilde{P}_l^d},\\(P_i^{\max},\frac{\sigma^2\tilde{P}_l^d}{r_l}),\quad\text{if}\frac{P_i^{\max}}{\tilde{P}_i^c}\le\frac{\sigma^2}{r_l}\le\frac{P_l^{\max}}{\tilde{P}_l^d},\\0,\qquad\qquad\text{otherwise.}\end{cases}\tag{9}$$

B. Phase Shift Optimization Subproblem

Given the variables $\mathbf{P}$ and $\mathbf{Z}$, we optimize the phase shift matrix $\mathbf{E}$ in this subsection. To facilitate the following optimization, we first convert some channel parameters. Let $\mathbf{e}=[e_1,\cdots,e_R]^T$ be the vector containing the diagonal elements of matrix $\mathbf{E}$ and $\mathbf{D}_{i,r}=\text{diag}(\mathbf{h}_{\text{i,r}})$ be the matrix diagonalized by vector. Hence, the V2I channel h_i^B is reformulated as

$$\begin{aligned}h_i^B&=\left|h_{i,b}+\mathbf{h}_{r,b}^H\mathbf{E}\mathbf{h}_{i,r}\right|^2=\left|h_{i,b}+\mathbf{h}_{r,b}^H\mathbf{D}_{i,r}\mathbf{e}\right|^2\\&=[a,\mathbf{e}^H][h_{i,b},\mathbf{h}_{r,b}^H\mathbf{D}_{j,r}]^H[h_{i,b},\mathbf{h}_{r,b}^H\mathbf{D}_{i,r}][a,\mathbf{e}^H]^H\\&=\text{Tr}\left(\mathbf{h}_{i,B}\mathbf{h}_{i,B}^H\mathbf{\Phi}\right)=\text{Tr}\left(\mathbf{H}_{i,B}\mathbf{\Phi}\right),\end{aligned}\tag{10}$$

where $\mathbf{h}_{i,B}=[h_{i,b},\mathbf{h}_{r,b}^H\mathbf{D}_{j,r}]^H\in\mathbb{C}^{(R+1)\times1}$, $\mathbf{H}_{i,B}=\mathbf{h}_{i,B}\mathbf{h}_{i,B}^H$, $\mathbf{\Phi}=[a,\mathbf{e}^H]^H[a,\mathbf{e}^H]$, a is an auxiliary variable and $|a|=1$. Likewise, the crosstalk channel h_l^B is reformulated as

$$h_l^B=\text{Tr}\left(\mathbf{h}_{l,B}\mathbf{h}_{l,B}^H\mathbf{\Phi}\right)=\text{Tr}\left(\mathbf{H}_{l,B}\mathbf{\Phi}\right),\tag{11}$$

where $\mathbf{h}_{l,B}=[h_{l,b},\mathbf{h}_{r,b}^H\mathbf{D}_{l,r}]^H$ and $\mathbf{D}_{l,r}=\text{diag}(\mathbf{h}_{\text{l,r}})$. Due to the non-concavity of the objective function, we apply the Successive Convex Approximation method to approximate the objective function. Because the first Taylor-expansion of any concave function at an point is its globally upper-bounded, for a given point $\mathbf{\Phi}^{(t)}$, the objective function is approximated as

$$C_{i,l}=Wf_i(\mathbf{\Phi})–Wf_l(\mathbf{\Phi})\ge Wf_i(\mathbf{\Phi})–Wf_l^{ub}(\mathbf{\Phi})=C_l^{lb},\tag{12}$$

where $f_i(\mathbf{\Phi})=\log_2\left(P_l^d\text{Tr}\left(\mathbf{H}_{l,B}\mathbf{\Phi}\right)+P_i^c\text{Tr}\left(\mathbf{H}_{i,B}\mathbf{\Phi}\right)+\sigma^2\right)$, $f_l(\mathbf{\Phi})=\log_2\left(P_l^d\text{Tr}\left(\mathbf{H}_{l,B}\mathbf{\Phi}\right)+\sigma^2\right)$ and $f_l^{ub}(\mathbf{\Phi})=f_l(\mathbf{\Phi}^{(t)})+\frac{P_l^d\text{Tr}\left(\mathbf{H}_{l,B}\left(\mathbf{\Phi}-\mathbf{\Phi}^{(t)}\right)\right)}{\left(P_l^d\text{Tr}\left(\mathbf{H}_{l,B}\mathbf{\Phi}^{(t)}\right)+\sigma^2\right)\ln2}$. By the above approximation, the objective function has been converted into the concave function and the phase shift optimization subproblem is reformulated as

$$\max_{\mathbf{\Phi}}\quad C_l^{lb}\tag{13}$$

$$\text{s.t.}\quad\Pr\left\{\frac{P_l^dh_l^d}{P_i^ch_i^d+\sigma^2}\ge\gamma_{th}\right\}\ge1-\delta,\tag{13a}$$

$$\mathbf{\Phi}_{[r,r]}=1,\ r=1,\cdots,R+1.\tag{13b}$$

Then, a useful lemma on the transformation outage probability constraint using the worst-case conditional value-at-risk (CVaR) approximation is given as follows:

Lemma 1. *Let $f(x)\in\mathbb{C}$, $\mathbf{f}(x)\in\mathbb{C}^{k\times1}$ and $\mathbf{F}(x)\in\mathbb{H}^k$ be the function with the variable $x\in\mathbb{R}$, where $\mathbb{H}$ is a hermitian matric. Suppose there exists a outage probability constraint denoted as*

$$\Pr\{f(x)+\mathbf{f}(x)^H\mathbf{h}+\mathbf{h}^H\mathbf{F}(x)\mathbf{h}\le0\}\ge1-\delta,\tag{14}$$

where $\mathbf{h}\in\mathbb{C}^{\mathbf{k\times1}}$ is a random vector. Then, (14) can be approximated as

$$\begin{cases}\alpha+\frac{1}{\delta}\text{Tr}\left(\mathbf{\Omega N}\right)\le0,\alpha\in\mathbb{R},\mathbf{N}\in\mathbb{H}^{(k+1)},\mathbf{N}\succeq0,\\\mathbf{N}-\begin{bmatrix}\mathbf{F}(x)&\frac{1}{2}\mathbf{f}(x)\\\frac{1}{2}\mathbf{f}(x)^H&f(x)-\alpha\end{bmatrix}\succeq0,\end{cases}$$

where α is an auxiliary variable, $\mathbf{N}$ is a matrix of auxiliary variables and $\mathbf{\Omega}$ is the second-order moment matrix of $\mathbf{h}$.

Proof: Refer to Section II in [14]. ■

Since the CVaR can approximate the chance constraint if the function in the chance constraint is a quadratic function of the random variables. To be compatible with Lemma 1, we convert the V2V channel as follows

$$h_l^d=\left|h_l+\mathbf{h}_{r,l}^H\mathbf{E}\mathbf{h}_{l,r}\right|^2=\left|h_l+\mathbf{h}_{r,l}^H\mathbf{D}_{l,r}\mathbf{e}\right|^2=\mathbf{h}_{l,d}^H\mathbf{\Phi}\mathbf{h}_{l,d},\tag{15}$$

where $\mathbf{h}_{l,d}=[h_l,\mathbf{h}_{r,l}^H\mathbf{D}_{l,r}]^H\in\mathbb{C}^{(R+1)\times1}$. Similarly, $h_i^d=\mathbf{h}_{i,d}^H\mathbf{\Phi}\mathbf{h}_{i,d}$, where $\mathbf{h}_{i,d}=[h_{i,l},\mathbf{h}_{r,l}^H\mathbf{D}_{i,r}]^H\in\mathbb{C}^{(R+1)\times1}$. Hence, the received SINR at the lth VUE can be converted into

$$\frac{P_l^dh_l^d}{P_i^ch_i^d+\sigma^2}\ge\gamma_{th}\Rightarrow P_l^dh_l^d-\gamma_{th}P_i^ch_i^d\ge\gamma_{th}\sigma^2\tag{16}$$

$$\Rightarrow\begin{bmatrix}\mathbf{h}_{l,d}^H&\mathbf{h}_{i,d}^H\end{bmatrix}\underbrace{\begin{bmatrix}P_l^d\mathbf{\Phi}&\mathbf{0}\\\mathbf{0}&-\gamma_{th}P_i^c\mathbf{\Phi}\end{bmatrix}}_{\mathbf{\Psi}\in\mathbb{C}^{2(R+1)}}\underbrace{\begin{bmatrix}\mathbf{h}_{l,d}\\\mathbf{h}_{i,d}\end{bmatrix}}_{\mathbf{h}_d\in\mathbb{C}^{(2R+2)\times1}}\ge\gamma_{th}\sigma^2,$$

which is a quadratic function of the uncertain channel $\mathbf{h}_d$. In order to learning the probability distribution information, the multiple samples of the uncertain CSI $\mathbf{h}_d$ are collected as $\mathcal{M}_d=\{\boldsymbol{\eta}_1^d,\boldsymbol{\eta}_2^d,\cdots,\boldsymbol{\eta}_M^d\}$, where $\boldsymbol{\eta}_m^d\in\mathbb{C}^{(2R+2)\times1}$. Thus, the mean vector and the covariance matrix of samples can be represented as $\bar{\boldsymbol{\eta}}_d=\frac{1}{M}\sum_{m=1}^M\boldsymbol{\eta}_m^d$ and $\mathbf{\Sigma}^d=\frac{1}{M}\sum_{m=1}^M(\boldsymbol{\eta}_m^d-\bar{\boldsymbol{\eta}}_d)(\boldsymbol{\eta}_m^d-\bar{\boldsymbol{\eta}}_d)^H$, respectively. The second-order moment matrix of $\mathbf{h}_d$ is represented as

$$\mathbf{\Omega}_d=\begin{bmatrix}\mathbf{\Sigma}^d+\bar{\boldsymbol{\eta}}_d\bar{\boldsymbol{\eta}}_d^H&\bar{\boldsymbol{\eta}}_d\\\bar{\boldsymbol{\eta}}_d^H&1\end{bmatrix}\in\mathbb{C}^{2R+3}.\tag{17}$$

Based on Lemma 1 and the above analyses, problem (13) can be reformulated as

$$\max_{\mathbf{\Phi},\mathbf{N}\in\mathbb{H}^{\mathbf{2R+3}},\alpha\in\mathbb{R}}\quad C_l^{lb}\tag{18}$$

$$\text{s.t.}\ \alpha+\frac{1}{\delta}\text{Tr}\left(\mathbf{\Omega_dN}\right)\le0,\mathbf{N}\succeq0,\ \mathbf{N}+\mathbf{\Delta}\succeq0,\mathbf{\Phi}\succeq0,\tag{18a}$$

$$\mathbf{\Phi}_{[r,r]}=1,\ r=1,\cdots,R+1,\tag{18b}$$

where $\mathbf{\Delta}=\begin{bmatrix}\mathbf{\Psi}&\mathbf{0}\\\mathbf{0}&\alpha-\gamma_{th}\sigma^2\end{bmatrix}\in\mathbb{H}^{2R+3}$, the unit-modulus constraint is converted into a tractable constraint in (18b). Therefore, problem (18) is a convex SDP problem and can be solved by CVX tools. The optimal solution $\mathbf{\Phi}^*$ to problem (18) can be decomposed to obtain the optimal $\mathbf{e}^*$ by the Gaussian randomization method [15] if $a=1$. If $a=-1$, obtaining the inverse $\mathbf{e}^*$ is equivalent to obtaining the optimal phase shifts.

C. Spectrum Allocation Subproblem

According to the above the power allocation and the phase shift optimization approaches, we can obtain the power solutions and the phase shift solutions based on all possible spectrum reusing pairs. Then, the Hungarian algorithm can be employed to obtain the optimal spectrum allocation solution. We assume that the number of CUEs is equal to the number of

VUEs, i.e., $I = L$. Hence, the spectrum allocation subproblem is formulated as

$$\max_{\mathbf{Z}} \quad \sum_{i\in\mathcal{I}}\sum_{l\in\mathcal{L}} z_{i,l}C_{i,l} \quad \text{s.t. (1c), (1d)}, \tag{19}$$

which is a bipartite matching problem in graph and can be resolved by the Hungarian algorithm.

D. Computational Complexity

Algorithm 1 Learning-based Alternating Optimization (LAOA) Algorithm

---

Initialize $\mathbf{P}^{(0)}$ and $\mathbf{E}^{(0)}$, and set the iterative index $t=0$.
for $i = 1, \cdots, I$ **do**
  for $l = 1, \cdots, L$ **do**
    repeat
      Solve problem (9) for given $\mathbf{E}^{(t)}$ and represent the optimal solution as $\mathbf{P}^{(t+1)}$;
      Solve problem (18) for given $\mathbf{P}^{(t+1)}$ and represent the optimal solution as $\mathbf{E}^{(t+1)}$;
      $t = t + 1$;
    until The change of the objective value is below a threshold $\varsigma = 10^{-3}$;
    The optimal capacity of the possible spectrum reusing pair $C_{i,l}$ is obtained;
  end for
end for
Apply Hungarian algorithm to compute the optimal spectrum reusing pattern $\mathbf{Z}^*$ based on $\{C_{i,l}\}$ and return the optimal resource allocation $\{\mathbf{P}^*, \mathbf{E}^*, \mathbf{Z}^*\}$.

In this subsection, we summarize the learning-based alternating optimization algorithm for RIS-aided V2X communications in **Algorithm 1** and discuss its computational complexity. Since we can obtain the closed-form solution of the power allocation subproblem that only needs some multiplication operations, its complexity is $\mathcal{O}_1 = \mathcal{O}(1)$. The complexity of problem (18) is $\mathcal{O}_2 = \mathcal{O}\Big((6R+9)^{1/2}u\big(u^2+u(R+2+2v^2+s^2)+R+2+2v^3+s^3\big)\Big)$, where $u = s^2 + v^2 + 1$, $v = 2R + 3$ and $s = R + 1$. The complexity of the Hungarian algorithm is $\mathcal{O}(I^3)$. Therefore, the complexity of the resource allocation problem is $\mathcal{O}\left(I^3 + I^2 t_{\max}\left(\mathcal{O}_1 + \mathcal{O}_2\right)\right)$, where $t_{\max}$ represents as the maximum number of iterations.

IV. Simulation Results

This section provides simulation results to evaluate the performance of our proposed approach. Fig.1 shows a RIS-aided vehicular network, where the coordinates of gNB and RIS are set as $(0\text{m}, 0\text{m}, 20\text{m})$ and $(80\text{m}, 0\text{m}, 20\text{m})$, respectively. There are 4 CUEs uniformly distributed on a circle centred at $(120\text{m}, 0\text{m}, 0\text{m})$ with a radius of 20m. Similarly, there are 4 VUE pairs randomly generated in a circle centred at $(140\text{m}, 130\text{m}, 0\text{m})$ with a radius of 70m. The pathloss exponents of gNB-vehicle, RIS-vehicle and gNB-RIS links are set as 4, 2 and 2.2, respectively. The small scale fading

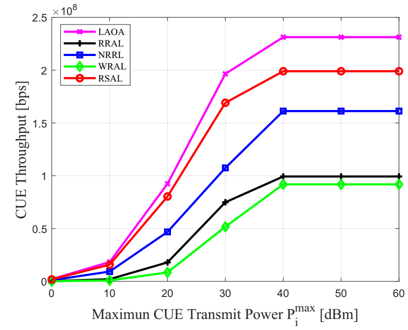

Fig. 3. CUE throughput versus the maximum CUE transmit power.

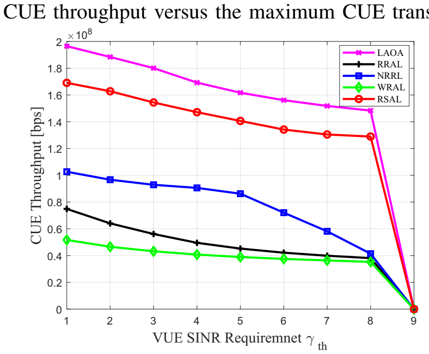

Fig. 4. CUE throughput versus the minimum VUE SINR requirement.

is considered as Rayleigh fading distribution. The channel correlation coefficient κ is the same as in [9]. In addition, the total number of RIS reflecting elements is $R = 20$. The other parameters are set as follows: $P_i^{\max} = P_l^{\max} = 30\text{dBm}$, $\text{W} = 10\text{MHz}$, $\sigma^2 = -114\text{dBm}$, $\delta = 0.01$, $\gamma_{th} = 1$ and $M = 1000$. For comparison, we simulate several baselines including a non-robust resource allocation method denoted as NRRL, a random RIS phase shifts method denoted as RRAL, a random spectrum allocation method denoted as RSAL and a method without RIS assistance denoted as WRAL.

Fig. 3 shows the impact of the maximum transmit power $P_i^{\max}$ on CUE throughput. It can be observed that when $P_i^{\max} = 0\text{dBm}$, CUE throughput is very small. As $P_i^{\max}$ is increased, CUE throughput starts to increase. When $P_i^{\max} \geq 40\text{dBm}$, the systems cannot allocate larger transmit power to CUE so that CUE throughput remains stable. This is because larger CUE transmit power will cause more interference to VUEs and can lead to the violation of the VUE QoS requirement. We also observed that CUE throughput of RSAL and NRRA is smaller than that of our proposed LAOA. This is because the spectrum allocation of RSAL is not optimal and NRRA can result in some samples of the uncertain channels violating the outage constraint. Furthermore, the performance of WRAL is the lowest and the performance of RRAL is slightly better than that of WRAL, which highlights the significance of RIS phase shifts optimization because the phase shift optimization solution of RRAL is not optimal and WRAL does not have RIS-assisted vehicular communication.

Fig. 4 compares CUE throughput versus the minimum VUE SINR requirement under different schemes. It can be seen that CUE throughput reduces as the minimum VUE SINR requirement γ_{th} increases. The reason is that a higher VUE SINR requirement results in the system allocating larger VUE

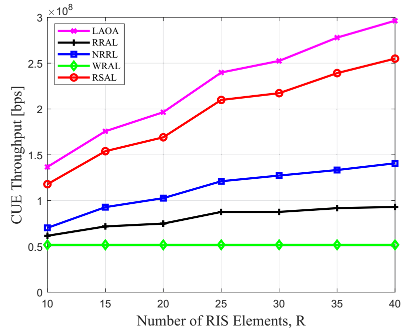

Fig. 5. CUE throughput versus the number of RIS reflecting elements R.

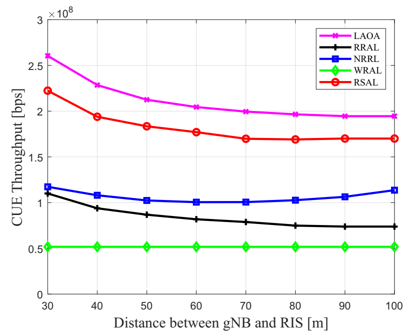

Fig. 6. CUE throughput versus the distance between gNB and RIS.

transmit power to satisfy the outage probability constraint. However, the increase of VUE transmit power will cause more interference to CUE, which reduces CUE throughput. When $\gamma_{th} \geq 8$, CUE throughput decreases to 0. The reason is that the system cannot allocate larger VUE transmit power due to the constraint of the maximum VUE transmit power. Therefore, the minimum VUE SINR requirement is no longer satisfied and the resource allocation problem becomes infeasible.

In Fig. 5, we illustrate CUE throughput versus the number of RIS reflecting elements. We find that the curves of all RIS-aided approaches rises with R, with the exception of WRAL's curve. The reason is that more RIS reflecting elements can form a larger reflective area and reflect more signal power, which leads to larger power gain. The curve of WRAL remains unchanged because WRAL considers the resource allocation problem for V2X communication without RIS support.

Fig. 6 plots CUE throughput versus the distance between gNB and RIS, where the variation of the distance depends on the variation of the RIS coordinate x_{RIS}. The distance between gNB and the centre of CUEs is set to approximately 130m. We observe that CUE throughput of NRRL first decreases and then starts to increase at 70m as the distance between gNB and RIS increases. This phenomenon can be explained in the following way, where the small scale fading is ignored for simplicity. Then, the large scale fading of the combined gNB-RIS-CUE channel can be formulated as $\sqrt{\omega_{i,b}} = \sqrt{\lambda (d_{i,b})^4 + \sqrt{\lambda^2 (d_{i,r})^2 (d_{r,b})^{2.2}}}$, where $d_{i,b} \approx d_{i,r} + d_{r,b}$. Thus, when $d_{i,b} = 2d_{i,r} = 2d_{r,b}$, the combined channel gain reaches the minimum value. Moreover, the CUE throughput of LAOA, RSAL and RRAL first decreases and then remains stable. The reason is that these methods all consider CSI uncertainty, which hinders the improvement of system performance as the distance grows.

V. Conclusions

In this paper, we investigated the issue of robust resource allocation in RIS-aided V2X communications, taking into account the uncertain partial vehicle channel CSI due to the Doppler effect. The sum capacity of CUEs maximization problem was formulated subject to the outage probability constraints of VUEs and RIS phase shifts. We presented a learning-based alternating optimization approach, which decomposed the problem into three subproblems to be iteratively optimized. Simulation results demonstrated that the proposed approach outperformed other benchmark methods, especially when compared to a vehicular network without RIS assistance.

References

[1] K. Ganesan, J. Lohr, P. B. Mallick, A. Kunz, and R. Kuchibhotla, "NR sidelink design overview for advanced V2X service," *IEEE Internet Things Mag.*, vol. 3, no. 1, pp. 26–30, 2020.

[2] Q. Wu and R. Zhang, "Intelligent reflecting surface enhanced wireless network via joint active and passive beamforming," *IEEE Trans. Wirel. Commun.*, vol. 18, no. 11, pp. 5394–5409, 2019.

[3] C. Huang, A. Zappone, G. C. Alexandropoulos, M. Debbah, and C. Yuen, "Reconfigurable intelligent surfaces for energy efficiency in wireless communication," *IEEE Trans. Wirel. Commun.*, vol. 18, no. 8, pp. 4157–4170, 2019.

[4] X. Yu, D. Xu, Y. Sun, D. W. K. Ng, and R. Schober, "Robust and secure wireless communications via intelligent reflecting surfaces," *IEEE J. Sel. Areas Commun.*, vol. 38, no. 11, pp. 2637–2652, 2020.

[5] M. D. Renzo, M. Debbah, D.-T. Phan-Huy, A. Zappone, M.-S. Alouini, C. Yuen, V. Sciancalepore, G. C. Alexandropoulos, J. Hoydis, H. Gacanin *et al.*, "Smart radio environments empowered by reconfigurable AI meta-surfaces: An idea whose time has come," *EURASIP J Wirel Commun Netw*, vol. 2019, no. 1, pp. 1–20, 2019.

[6] Y. Chen, Y. Wang, J. Zhang, and Z. Li, "Resource allocation for intelligent reflecting surface aided vehicular communications," *IEEE Trans. Veh. Technol.*, vol. 69, no. 10, pp. 12 321–12 326, 2020.

[7] S. Jia, X. Yuan, and Y.-C. Liang, "Reconfigurable intelligent surfaces for energy efficiency in D2D communication network," *IEEE Wireless Commun. Lett.*, vol. 10, no. 3, pp. 683–687, 2020.

[8] Y. Chen, Y. Wang, J. Zhang, and M. Di Renzo, "QoS-driven spectrum sharing for reconfigurable intelligent surfaces (RISs) aided vehicular networks," *IEEE Trans. Wirel. Commun.*, vol. 20, no. 9, pp. 5969–5985, 2021.

[9] W. Wu, R. Liu, Q. Yang, and T. Q. Quek, "Robust resource allocation for vehicular communications with imperfect CSI," *IEEE Trans. Wirel. Commun.*, vol. 20, no. 9, pp. 5883–5897, 2021.

[10] J. Cheng, C. Shen, Z. Chen, and N. Pappas, "Robust Beamforming Design for IRS-Aided URLLC in D2D Networks," *IEEE Trans Commun*, vol. 70, no. 9, pp. 6035–6049, 2022.

[11] G. Zhou, C. Pan, H. Ren, K. Wang, and A. Nallanathan, "A framework of robust transmission design for IRS-aided MISO communications with imperfect cascaded channels," *IEEE Trans. Signal Process.*, vol. 68, pp. 5092–5106, 2020.

[12] Z. Peng, Z. Chen, C. Pan, G. Zhou, and H. Ren, "Robust transmission design for RIS-aided communications with both transceiver hardware impairments and imperfect CSI," *IEEE Wireless Commun. Lett.*, vol. 11, no. 3, pp. 528–532, 2021.

[13] T. Kim, D. J. Love, and B. Clerckx, "Does frequent low resolution feedback outperform infrequent high resolution feedback for multiple antenna beamforming systems?" *IEEE Trans. Signal Process.*, vol. 59, no. 4, pp. 1654–1669, 2010.

[14] S. Zymler, D. Kuhn, and B. Rustem, "Distributionally robust joint chance constraints with second-order moment information." *Math Program*, vol. 137, 2013.

[15] Q. Wu and R. Zhang, "Intelligent reflecting surface enhanced wireless network: Joint active and passive beamforming design," in *2018 IEEE Global Commun. Conf. (GLOBECOM)*. IEEE, 2018, pp. 1–6.